# The C-terminal calcium-sensitive disordered motifs regulate isoform-specific polymerization characteristics of calsequestrin

**Naresh C. Bal[1],[\*], Nivedita Jena[2], Harapriya Chakravarty[3], Amit Kumar[4], Mei Chi[1], Tuniki Balaraju[3], Sharad V. Rawale[5], Jayashree S. Rawale[5], Ashoke Sharon[3], and Muthu Periasamy[1]**

[1]Department of Physiology and Cell Biology, College of Medicine, The Ohio State University, Columbus, OH 43210, United States

[2]College of Pharmacy, The Ohio State University, Columbus, OH 43210, United States

[3]Department of applied Chemistry, Birla Institute of Technology, Mesra, Ranchi, Jharkhand 835215, India

[4]Department of Biomedical Sciences, University of Cagliari, Cagliari 09124, Italy

[5]Ohio Peptide LLC, Powell, OH 43065

## Abstract

Calsequestrin (CASQ) exists as two distinct isoforms CASQ1 and CASQ2 in all vertebrates. Although the isoforms exhibit unique functional characteristic, the structural basis for the same is yet to be fully defined. Interestingly, the C-terminal region of the two isoforms exhibit significant differences both in length and amino acid composition; forming Dn-motif and DEXn-motif in CASQ1 and CASQ2 respectively. Here, we investigated if the unique C-terminal motifs possess $Ca^{2+}$-sensitivity and affect protein function. Sequence analysis shows that both the Dn- and DEXn-motifs are intrinsically disordered regions (IDRs) of the protein, a feature that is conserved from fish to man. Using purified synthetic peptides, we show that these motifs undergo distinctive $Ca^{2+}$-mediated folding suggesting that these disordered motifs are $Ca^{2+}$-sensitivity. We generated chimeric proteins by swapping the C-terminal portions between CASQ1 and CASQ2. Our studies show that the C-terminal portions do not play significant role in protein folding. An interesting finding of the current study is that the switching of the C-terminal portion completely reverses the polymerization kinetics. Collectively, these data suggest that these $Ca^{2+}$-sensitivity IDRs located at the back-to-back dimer interface influence isoform-specific $Ca^{2+}$-dependent polymerization properties of CASQ.

## Keywords

calcium binding protein; circular dichroism; disordered motifs; calcium-induced polymerization

---

[\*]Address correspondence to: Naresh Bal, 102 Hamilton Hall, 1645 Neil Ave, Columbus, OH 43210. Fax: 614-292-4888; bal. 8@osu.edu.

## INTRODUCTION

Calsequestrin (CASQ) is a high capacity $Ca^{2+}$-binding protein, critical for $Ca^{2+}$-buffering in cardiac and skeletal muscle sarcoplasmic reticulum (SR) [1–6]. All vertebrates including humans have two isoforms of CASQ with differential expression pattern; **CASQ1** is expressed primarily in fast twitch skeletal muscle, while **CASQ2** is expressed in the cardiac and slow twitch muscle [1,3,7–11]. Studies suggest that CASQ1 and CASQ2 differ significantly in their $Ca^{2+}$ buffering capacity; CASQ1 binds more $Ca^{2+}$ (~70–80 $Ca^{2+}$/molecule) than CASQ2 (~50–60 $Ca^{2+}$/molecule) [12], which indicates that CASQ1 has a higher capacity to store and buffer $Ca^{2+}$. Further, CASQ1 is shown to polymerize at 0.5 mM $Ca^{2+}$ whereas CASQ2 remains monomeric indicating differences in their $Ca^{2+}$-mediated polymerization dynamics [6,12]. In addition to maintaining SR $Ca^{2+}$-content, CASQ is shown to interact and regulate the gating behavior of the ryanodine receptor (RyR) and thereby controlling $Ca^{2+}$-release from the SR that is unique to the muscle type [5–6,13–16]. Recent studies using reconstituted RyR systems in lipid bilayers, suggest that CASQ isoforms interact with RyR isoforms and modulate RyR function very differently [5–6]. Therefore, all these studies suggest that CASQ1 and CASQ2 have unique functional differences.

The structural basis for the functional differences between the CASQ isoforms has not been fully defined. The structures determined for the two proteins, showed that CASQ1 and CASQ2 have very similar 3-Dimensional (3D) folding, however the CASQ1 surface is much more negatively charged than CASQ2 [12]. Based on structural studies, Park et al proposed a $Ca^{2+}$-mediated polymerization model that could be applied to both CASQ1 and CASQ2 isoforms [17]. The recently solved structure for CASQ1 in hexameric state provide validation for the model and existence of linear polymer [18]. In this model, CASQ exists as a random coil at very low $Ca^{2+}$ concentration. As the $Ca^{2+}$ concentration increases the molecules fold into a compact monomer and at first two monomers form front-to-front dimers by exchange of extended N-terminal residues. Subsequently, two dimers establish back-to-back stacking to form tetramers, finally leading to formation of linear polymers. The back-to-back interface is not stabilized by exchange of any motifs and only few residue-to-residue interactions were observed, suggesting that the CASQ polymer may be very fragile. Therefore, the tetramerization by back-to-back stacking may be a critical step in the $Ca^{2+}$-dependent polymerization dynamics of CASQ.

The C-terminal residues that occur near the back-to-back interface may influence the tetramerization process. However, the X-ray diffraction could not resolve the coordinates for these C-terminal residues [19] and it is currently unknown if it can affect the isoform specific functions. Our recent computational study showed that C-terminus of CASQ1 undergoes coiling upon $Ca^{2+}$-binding indicating that these residues may be a $Ca^{2+}$-sensitive motif [20]. Studies have shown that deletion of the C-terminal residues does not affect CASQ localization [21–22], although other studies suggested that CASQ polymerization is essential for its localization to the SR [23–24]. Phosphorylation and glycosylation have also been proposed to be important for CASQ localization [24–28]. It is also interesting to note that, the C-terminus of CASQ2 exhibits higher rate of phosphorylation than CASQ1 [29–30]. All the above observations suggest that the distinct C-termini may be the basis of unique isoform-specific function of CASQ. Therefore, in this study we wanted to test if the unique C-

terminus is an important regulator of isoform specific polymerization of the CASQ1 and CASQ2. To test this possibility we created CASQ chimeras where the C-terminal portion of CASQ1 and CASQ2 proteins were swapped and examined how chimerization affect protein folding, and polymerization.

## RESULTS

### Ordered and disordered parts of CASQ isoforms show distinct sequence conservation pattern

To determine structural features that are unique to the CASQ1 or 2 isoforms, we analyzed evolutionary conservation of CASQ1 and CASQ2 proteins among 47 vertebrates including 27 mammalian species. Comparison between the two isoforms suggested that the body of the proteins (aa 1–345) is highly conserved across species within each individual CASQ isoform (Supplemental Figure 1). The pairwise alignment scores for CASQ1 sequence from frog (*Pelophylax esculentus*) and gray short-tailed opossum (*Monodelphis domestica*, a primitive marsupial mammal) against human CASQ1 was 85.8 and 95.8 respectively. There is also a moderate level of conservation between isoforms; the alignment scores for CASQ1 vs. CASQ2 in human and mouse was 67.3 and 68.8 respectively. Structural alignment further showed that the secondary structural elements and domain boundaries overlap between the isoforms (Supplemental Figure 1). Among individual domains, the domain III (aa 225–350; not considering C-terminal non-homologous residues) is highly conserved and this region shows about 95% homology between CASQ1 and CASQ2 in case of most of the species. Domain I and domain II exhibit homology of ~60% and ~70% respectively in most species. This sequence conservation pattern suggest that the folding pattern of CASQ1 and CASQ2 is very similar in all the vertebrate taxa, as suggested by Whittington et al [31]. In contrast, the C-terminal disordered region of CASQ1 and CASQ2 are not conserved across isoforms.

### CASQ isoforms possess unique intrinsically disordered motifs at C-terminus

A unique feature of CASQ is that the amino acid composition of the C-terminal region (aa 357- to -COOH) is strikingly different between the two isoforms (figure 1). The CASQ2 tail has non-acidic residues (usually Asn, Ser, and Gly) repeated after every few acidic residues in all the species irrespective of the taxa. On the contrary, the CASQ1 tail possess only negative residues, mostly Asp and rarely Glu, without the presence of any non-acidic residues. This unique residue composition is strikingly conserved from fishes to human among both the CASQ1 and CASQ2 isoforms, which supports the recent proposition that the duplication of CASQ sequence giving rise to CASQ1 and CASQ2 must have occurred during early piscine evolution [32]. Based on the strict conservation of residue composition we designated, the C-terminal end of CASQ1 as Dn-motif ("Dn" represents a polymer of aspartic acids) and that of CASQ2 as DEXn-motif ("DEXn" represent a polymer of acidic residues with intermittent presence of non-acidic residues represented as "X"). Interestingly, our further analysis of CASQ sequences using intrinsically disordered regions (IDRs) predictor programs shows that both Dn and DEXn-motifs are IDRs (figure 1). All the prediction programs indicated that domain I, II and III of both CASQ isoforms from all the

taxa have low probability of containing IDRs, whereas unanimously indicated both Dn and DEXn-motifs as IDRs.

### Dn and DEXn-motifs are sensitive to $Ca^{2+}$-binding

Next, we tested the hypothesis that the Dn and DEXn-motifs are sensitive to $Ca^{2+}$ ions using purified synthetic peptides applying CD spectroscopy. Our CD data suggest that the Dn-motif in buffer with no additional $Ca^{2+}$ ions remains mostly in linear conformation, whereas the DEXn-motif contain some coils as indicated from negative peak observed at 208nm (figure 2A and B). Upon addition of $Ca^{2+}$, the Dn-motif underwent coiling as indicated by increase in absorbance at 208nm. Interestingly, DEXn-motif acquired both coiled and helical structures upon addition of $Ca^{2+}$, as it gains absorbance both at 222nm and at 208nm (figure 2B). The control peptides (CP) did not show any significant change in CD ellepticity suggesting that only Dn and DEXn peptides are sensitive to increase in $Ca^{2+}$-concentration. None of the four peptides studied form aggregates upon addition of $CaCl_2$, suggesting that the change in CD ellepticity upon increase in $Ca^{2+}$-concentration is due to the intrinsic properties of the Dn and DEXn peptides. Further, we plotted CD absorbance against $Ca^{2+}$-concentration to characterize the kinetics of structural change. As shown in figure 2C, Dn-motif acquires maximal coiling (ellepticity at 208nm) ~1.2 mM $Ca^{2+}$ and does not (ellepticity at 222nm) acquire much helical content. On the other hand figure 2D shows that the DEXn-motif acquires some helical content ~1 mM $Ca^{2+}$ and acquires coiled-structures progressively upto ~2 mM $Ca^{2+}$. These data suggest that the Dn and DEXn-peptides undergo distinct $Ca^{2+}$-induced folding.

### Swapping of C-terminal portions between CASQ1 and 2 does not impair protein folding

Next, we wanted to determine if C-terminal disordered motifs affect protein folding. We generated chimeric proteins by swapping the C-terminal portion between CASQ1 and CASQ2. We compared the mean residue ellipticity (MRE) of each chimera with the WT CASQ. Interestingly, both the chimeric proteins exhibited similar CD spectra compared to the CASQ1 and CASQ2 WT proteins (figure 3), suggesting that both chimeras can fold to similar conformation as the WT proteins. Further, we employed a computational approach to study if addition of C-terminal residues affected the gross protein structure. To analyze this two additional in-silico chimeras, apart from the CS and SC chimeras, were generated by swapping C-termini at the residue number 350. The additional in-silico chimeras are named; C-Sk (cardiac containing the Dn-motif) and S-Ca (skeletal containing the DEXn-motif). The C-Sk and S-Ca chimeras were generated to show that the residues from 250–350 do not drastically alter monomeric structure. After MD simulation and energy minimization, we found that all four chimeric structures (CS, SC, C-Sk, and S-Ca) remain folded to a similar conformation as that of the WT proteins (figure 4). The root mean square distance (RMSD) values calculated for the four chimeric structures with respect to average WT protein structure from MD simulations are (i) S-Ca: 1.4 Å (Fig. 4B) (ii) SC: 1.7 Å (Fig. 4C) (iii) C-Sk: 2.3 Å (Fig. 4E) and (iv) CS: 2.7 Å (Fig. 4F). Collectively these data suggest that swapping of the C-terminal residues either at position 250 or at 350 does not significantly alter protein folding.

### Chimerization reverses the polymerization kinetics of the CASQ1 and 2 isoforms

The Dn and DEXn-motifs are located at the interface of back-to-back dimer (Supplemental Figure 2), and could influence tetramerization thereby the polymerization kinetics of the CASQ isoforms. Therefore, we investigated if exchange of C-terminal portion affect CASQ polymerization property. We exposed purified CASQ proteins (both WT and chimeras) to increasing $Ca^{2+}$-concentrations and measured turbidity in the solution. Interestingly, our turbidimetric measurements with increasing $Ca^{2+}$-concentration shows that the CS-chimera polymerizes faster with less $Ca^{2+}$ than CASQ2 and the turbidimetric curve for CS-chimera is similar to that of CASQ1 (figure 5). Moreover, the SC-chimera polymerizes slower with more $Ca^{2+}$ than CASQ1 and its turbidimetric curve is similar to that of CASQ2. These data suggest that the DEXn-motif being bigger may causes greater hindrance to tetramerization affecting polymerization compared to the small Dn-motif.

## DISCUSSION

Recent studies suggest that CASQ is more than a $Ca^{2+}$ buffer and loss of CASQ2 affects RyR2 activity leading to cardiac arrhythmias [4,33–35]. However there is continued controversy whether CASQ2 and CASQ1 play unique functional roles in cardiac and skeletal muscle. Many published studies show that CASQ1 and CASQ2 isoforms differ in their $Ca^{2+}$-binding and polymerization properties [12,17,36–37] and in their ability to regulate RyR activity [5–6]. Comparison of crystals of the two CASQ isoforms showed that the secondary structural elements and tertiary structure are superimposable, but that their surface charge distribution is dissimilar; the CASQ1 being more negative than the CASQ2 [12]. However, the coordinates for the Dn and DEXn motifs has not been resolved in any of the published structure and their role in isoform specific function is not known. Our computational analysis showed that Dn-motif can undergo $Ca^{2+}$-induced coiling [20]. Further, the DEXn-motif of CASQ2 that possesses serine residues undergoes phosphorylation at much higher rate than the Dn-motif of CASQ1 [29], indicating role of these motifs in unique isoform-specific functions. Phosphorylation may add negative charge to the DEXn-motif and hinder back-to-back stacking and interaction with RYR2, that may affect $Ca^{2+}$-dynamics.

The most striking observation from this study is that the C-terminal portion of CASQ influence polymerization properties but not protein folding. Turbidity measurement shows that swapping of the C-terminal portion completely reverses the polymerization kinetics. Whereas, CD and computational data showed that the secondary structural folding is not impaired in the chimeric proteins, indicating the possibility they exist in a comparably folded state. Based on the current data and other published studies, we propose that the C-terminus of CASQ isoforms play a role in the back-to-back stacking especially tertramerization which is a rate-limiting step in linear polymerization. The Dn or DEXn-motif are present at the back-to-back interface and undergo distinct $Ca^{2+}$-dependent folding. Therefore, these motifs can uniquely regulate tetramerization due to tail-to-tail repulsion. The Dn-motif in CASQ1 (composed of ~10 Asp residues) needs less cation mediated neutralization. Whereas, the DEXn-motif of CASQ2 (composed of ~28 acidic residues), requires higher concentration of $Ca^{2+}$, in order to overcome the tail-to-tail charge repulsion

before back-to-back contacts can be established leading to formation of a tetramer. This interpretation is further supported by the fact that the CASQ1 is able to polymerize at a lower $Ca^{2+}$ (~0.7 mM) while CASQ2 needs much higher $Ca^{2+}$ (~2 mM) to become oligomerized/aggregated. It is also interesting that, the polymerized CASQ1 has a higher negative surface charge and therefore can bind and release more $Ca^{2+}$ [12,38]. On the other hand, CASQ2 binds lesser $Ca^{2+}$ (due to lower surface negativity) and the DEXn-motif requires more $Ca^{2+}$ for the charge neutralization before two CASQ2 dimers can establish tetramer by back-to-back stacking. The DEXn-motif may additionally play some role in stabilization of CASQ2 tetramer, as C-terminal truncation impairs polymerization [12]. We show data to indicate that disorder regions of CASQ, a calcium-buffering protein, acquire secondary structure upon increase in $Ca^{2+}$-concentration which suggest that these may work as unique $Ca^{2+}$-sensing motifs. Further, these motifs after their $Ca^{2+}$-induced folding can distinctly regulate $Ca^{2+}$-dependent polymerization of CASQ isoforms indicating that such motifs can be exploited by the nature to manipulate protein-protein interaction in $Ca^{2+}$-dependent manner. Such a regulation of cellular function can be of adaptive value as it may play a key role in using $Ca^{2+}$-ions as a second messenger in various cellular processes of striated muscles. We hope future research will define the role of Dn and DEXn motifs in RYR-CASQ interaction and in overall intracellular calcium dynamics. These observations may also suggest that the polymerization dynamics of CASQ2 is slow compared to CASQ1 which may provide functional advantages to slow and/or cardiac muscle.

## MATERIALS AND METHODS

### Protein Sequence Analysis

Protein sequences for CASQ1 and CASQ2 were compiled from various vertebrate species using the tBLASTn program on the NCBI server and sequence comparison analysis were performed as described previously [37]. Sequence conservation in the structural domain (aa 1–345) was determined by analyzing, 78 sequences from 47 vertebrate species that included 27 mammalian species. The accession numbers of sequences used are provided in the supplemental information. The analysis of intrinsically disordered regions (IDRs) in various CASQ sequences was carried out using online server, "DisProt" (http://www.disprot.org/metapredictor.php), which includes VSL2B, VL3, VLXT and PONDR-FIT analyses [39–40]. We additionally used other online IDRs prediction programs, DisEMBL™ [41] and IUPred [42].

### Peptide studies

The Dn (TEDDDDDDDDDDDDDDDDDDD) and DEXn (TEDDDNEDEDDDGDNDNDDDDDDDDNSDEDNDDSDDDDDDDDE) motif peptides were synthesized, purified, verified and provided by Ohio Peptide LLC, Powell, OH. In addition, peptides of similar sized but of different sequence (LYRNGKMEVGWYRSPFSRVVH and SLIKGVIVHRLEGVERSDGPSLYKFYEDKLLANGTRDHKK) were also provided and were used as controls. Structural changes in these peptides upon exposure to $Ca^{2+}$ was monitored using CD. CD was measured using same instrumentation parameters as above in two different buffers; either 5mM HEPES, 20mM NaCl, pH 7.5 or 10mM MOPS, 20mM NaCl, pH 7.5.

## Generation of CASQ Chimeras

The adenoviral constructs of CASQ1, CASQ2, CS-chimera containing N-terminal amino acids (aa) 1–249 of CASQ2 (the cardiac isoform) and C-terminal aa 250–370 of CASQ1 (the skeletal isoform) and SC-chimera containing N-terminal 1–249 aa of CASQ1 and C-terminal aa 250–394 of CASQ2 were generated. Rat cDNA of CASQ1 and CASQ2 were generated by PCR-driven amplification. Dra III restriction enzyme site was selected as site of exchange the tails of CASQ1 and CASQ2. This site was chosen for the swap because the secondary structural elements from aa 250 to aa 356 overlap and more than 90% residues are strictly conserved and may not affect protein folding.

## Circular Dichroism (CD) spectroscopy

The cloning, expression and purification of CASQ2 has been published by us earlier [43]. The CASQ1 and the SC-chimera were subcloned into pET21d vector (Novagen) between NcoI and XhoI restriction sites. The CS-chimera was subcloned into pET21a vector (Novagen) between NdeI and XhoI restriction sites. The proteins were expressed in bacterial cells and purified using earlier published method [37]. The conditions for over-expression and purification were individually optimized for each chimera to ensure maximum yield of the protein. CD spectra were acquired in 20 mM Tris buffer, pH 7.5, containing 300 mM NaCl using an Aviv spectropolarimeter, inside a temperature controlled cell holder [44]. All of the spectra were recorded at 25°C in triplicate from two different purification batches. The CD data was processed and expressed in mean residue ellipticity (MRE, deg. $cm^2$ $dmol^{-1}$) as described earlier [45].

## Computational studies

We first built models using coordinates from 3TRQ and 2AVF as the starting structures of all the four CASQ sequences (CASQ1, CASQ2, CS-chimera and SC-chimera). In the case of both the chimeras the structures the residues from 250–350 was used from the isoform it is coming from. The C-terminal residues that are missing in the crystal structure were added to all the four structures. Apart from these two chimeras we generated two more in-silico chimeras having swap at the residue number 350 named C-Sk (contain Dn-motif) and S-Ca (contain DEXn-motif). The models were built employing Prime module and then manually refined in Maestro module. The generated homology models were also analyzed through Ramachandran plot and procheck software and further corrected manually. Then, the energy minimized structures were subjected to molecular dynamics simulations employing NAMD software[46]. The WT and Chimeric structures of CASQ1 and CASQ2 proteins, were then inserted in the water box, and counter ions were added to neutralize the system, using VMD software[47]. We used CHARMM27 force field parameters for the protein[48] and TIP3P parameters for the water molecules. Each molecular system was then gradually heated to 300 K in steps of 30 K, constraining the C-alpha atoms to 50 kcal (mol/$Å^2$). The constraints on the C-alpha atoms were released in steps of 10 kcal(mol/$Å^2$). We then performed 3 ns of equilibration run. Production run of 10 ns for each system at 300 K and 1atm pressure (NPT ensemble), using periodic boundary conditions was performed. The simulations were performed for each system for a period of 10 ns at 300 K and 1 atm pressure (NPT

ensemble), using periodic boundary conditions. After the completion of MD simulation, an average structure for each of the system was used for analysis.

### Calcium-dependent polymerization

Calcium-induced polymerization of WT and chimeric proteins was monitored by adding aliquots (2–5 μl) of $CaCl_2$ from stock solutions (0.1–2 M) to a solution of 2.75 μM protein in 20 mM Tris buffer, pH 7.5, containing 20 mM NaCl. After addition of calcium, protein samples were mixed and incubated to equilibrate for at least 5 min, and then absorbance was recorded at 350 nm as described [44]. All turbidity measurements were repeated three times.

## Supplementary Material

Refer to Web version on PubMed Central for supplementary material.

## Acknowledgments

## References

1. Biral D, Volpe P, Damiani E, Margreth A. FEBS Lett. 1992; 299:175–178. [PubMed: 1544490]

2. Fliegel L, Leberer E, Green NM, MacLennan DH. FEBS Lett. 1989; 242:297–300. [PubMed: 2914612]

3. Froemming GR, Murray BE, Harmon S, Pette D, Ohlendieck K. Biochim Biophys Acta. 2000; 1466:151–168. [PubMed: 10825439]

4. Beard NA, Laver DR, Dulhunty AF. Prog Biophys Mol Biol. 2004; 85:33–69. [PubMed: 15050380]

5. Qin J, Valle G, Nani A, Chen H, Ramos-Franco J, Nori A, Volpe P, Fill M. Biophys J. 2009; 97:1961–1970. [PubMed: 19804727]

6. Wei L, Hanna AD, Beard NA, Dulhunty AF. Cell Calcium. 2009; 45:474–484. [PubMed: 19376574]

7. Damiani E, Volpe P, Margreth A. J Muscle Res Cell Motil. 1990; 11:522–530. [PubMed: 2084148]

8. Murphy RM, Larkins NT, Mollica JP, Beard NA, Lamb GD. J Physiol. 2009; 587:443–460. [PubMed: 19029185]

9. Park KW, Goo JH, Chung HS, Kim H, Kim DH, Park WJ. Gene. 1998; 217:25–30. [PubMed: 9795116]

10. Arai M, Alpert NR, Periasamy M. Gene. 1991; 109:275–279. [PubMed: 1662658]

11. Arai M, Otsu K, MacLennan DH, Periasamy M. Am J Physiol. 1992; 262:C614–620. [PubMed: 1372478]

12. Park H, Park IY, Kim E, Youn B, Fields K, Dunker AK, Kang C. J Biol Chem. 2004; 279:18026–18033. [PubMed: 14871888]

13. Restrepo JG, Weiss JN, Karma A. Biophys J. 2008; 95:3767–3789. [PubMed: 18676655]

14. Lee YS, Keener JP. J Theor Biol. 2008; 253:668–679. [PubMed: 18538346]

15. Gyorke I, Hester N, Jones LR, Gyorke S. Biophys J. 2004; 86:2121–2128. [PubMed: 15041652]

16. Ma J, Pan Z. Cell Calcium. 2003; 33:375–384. [PubMed: 12765683]

17. Park H, Wu S, Dunker AK, Kang C. J Biol Chem. 2003; 278:16176–16182. [PubMed: 12594204]

18. Sanchez EJ, Lewis KM, Danna BR, Kang C. J Biol Chem. 2012; 287:11592–11601. [PubMed: 22337878]

19. Gaburjakova M, Bal NC, Gaburjakova J, Periasamy M. Cellular and Molecular Life Sciences. 2013; 70:2935–2945. [PubMed: 23109100]

20. Kumar A, Chakravarty H, Bal NC, Balaraju T, Jena N, Misra G, Bal C, Pieroni E, Periasamy M, Sharon A. Molecular Biosystems. 2013; 9:1949–1957. [PubMed: 23629537]

21. Nori A, Gola E, Tosato S, Cantini M, Volpe P. Am J Physiol. 1999; 277:C974–981. [PubMed: 10564090]

22. Nori A, Nadalini KA, Martini A, Rizzuto R, Villa A, Volpe P. Am J Physiol. 1997; 272:C1420–1428. [PubMed: 9176130]

23. Cho JH, Ko KM, Singaruvelu G, Lee W, Kang GB, Rho SH, Park BJ, Yu JR, Kagawa H, Eom SH, Kim do H, Ahnn J. J Cell Sci. 2007; 120:1551–1558. [PubMed: 17405817]

24. Houle TD, Ram ML, McMurray WJ, Cala SE. Exp Cell Res. 2006; 312:4150–4161. [PubMed: 17045261]

25. Gatti G, Trifari S, Mesaeli N, Parker JM, Michalak M, Meldolesi J. J Cell Biol. 2001; 154:525–534. [PubMed: 11489915]

26. Milstein ML, Houle TD, Cala SE. Exp Cell Res. 2009; 315:523–534. [PubMed: 19059396]

27. Nori A, Valle G, Massimino ML, Volpe P. Exp Cell Res. 2001; 265:104–113. [PubMed: 11281648]

28. Nori A, Furlan S, Patiri F, Cantini M, Volpe P. Exp Cell Res. 2000; 260:40–49. [PubMed: 11010809]

29. Cala SE, Jones LR. J Biol Chem. 1991; 266:391–398. [PubMed: 1985907]

30. Scott BT, Simmerman HK, Collins JH, Nadal-Ginard B, Jones LR. J Biol Chem. 1988; 263:8958–8964. [PubMed: 3379055]

31. Whittington AC, Nienow TE, Whittington CL, Fort TJ, Grove TJ. PLoS One. 2012; 7:e50801. [PubMed: 23226387]

32. Infante C, Ponce M, Manchado M. Comp Biochem Physiol B Biochem Mol Biol. 2011; 158:304–314. [PubMed: 21256971]

33. Szegedi C, Sarkozi S, Herzog A, Jona I, Varsanyi M. Biochem J. 1999; 337(Pt 1):19–22. [PubMed: 9854019]

34. Launikonis BS, Zhou J, Royer L, Shannon TR, Brum G, Rios E. Proc Natl Acad Sci U S A. 2006; 103:2982–2987. [PubMed: 16473932]

35. Royer L, Sztretye M, Manno C, Pouvreau S, Zhou J, Knollmann BC, Protasi F, Allen PD, Rios E. J Gen Physiol. 2010; 136:325–338. [PubMed: 20713548]

36. Ikemoto N, Nagy B, Bhatnagar GM, Gergely J. J Biol Chem. 1974; 249:2357–2365. [PubMed: 4856651]

37. Bal NC, Sharon A, Gupta SC, Jena N, Shaikh S, Gyorke S, Periasamy M. J Biol Chem. 2010; 285:17188–17196. [PubMed: 20353949]

38. Murphy RM, Mollica JP, Beard NA, Knollmann BC, Lamb GD. Am J Physiol Heart Circ Physiol. 2011; 300:H595–604. [PubMed: 21131479]

39. Obradovic Z, Peng K, Vucetic S, Radivojac P, Dunker AK. Proteins. 2005; 61(Suppl 7):176–182. [PubMed: 16187360]

40. Xue B, Dunbrack RL, Williams RW, Dunker AK, Uversky VN. Biochim Biophys Acta. 2010; 1804:996–1010. [PubMed: 20100603]

41. Linding R, Jensen LJ, Diella F, Bork P, Gibson TJ, Russell RB. Structure. 2003; 11:1453–1459. [PubMed: 14604535]

42. Dosztanyi Z, Csizmok V, Tompa P, Simon I. Bioinformatics (Oxford, England). 2005; 21:3433–3434.

43. Kalyanasundaram A, Bal NC, Franzini-Armstrong C, Knollmann BC, Periasamy M. J Biol Chem. 2010; 285:3076–3083. [PubMed: 19920148]

44. Bal NC, Jena N, Sopariwala D, Balaraju T, Shaikh S, Bal C, Sharon A, Gyorke S, Periasamy M. Biochem J. 2011; 435:391–399. [PubMed: 21265816]

45. Bal NC, Agrawal H, Meher AK, Arora A. Biol Chem. 2007; 388:467–479. [PubMed: 17516842]

46. Phillips JC, Braun R, Wang W, Gumbart J, Tajkhorshid E, Villa E, Chipot C, Skeel RD, Kale L, Schulten K. J Comput Chem. 2005; 26:1781–1802. [PubMed: 16222654]

47. Humphrey W, Dalke A, Schulten K. J Mol Graph. 1996; 14:33–38. 27–38. [PubMed: 8744570]

48. MacKerell AD Jr, Banavali N, Foloppe N. Biopolymers. 2000; 56:257–265. [PubMed: 11754339]
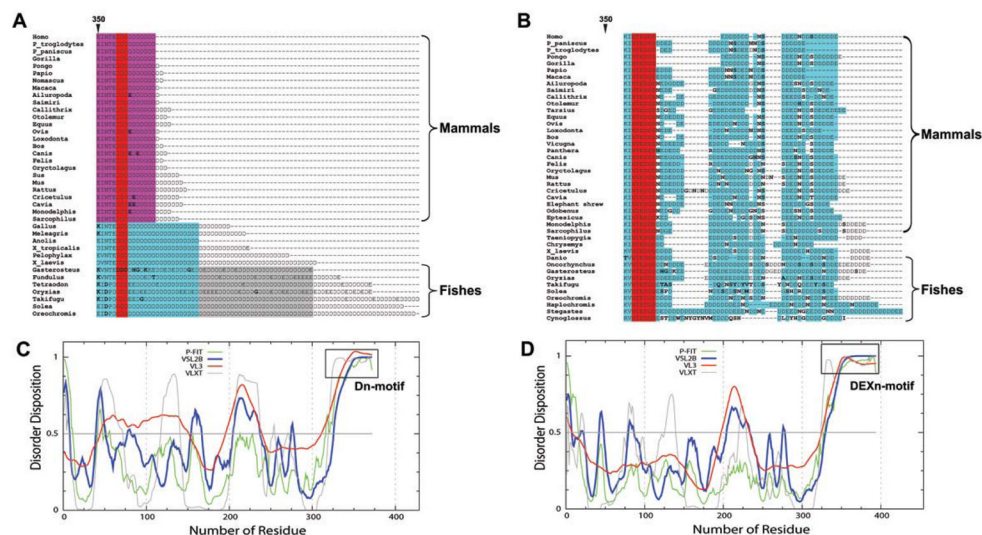
**Figure 1. The C-terminal tail is distinctly different between CASQ isoforms**

Multiple sequence alignment of the C-terminal residues of various CASQ sequences from all the species. Alignment of the whole protein is presented in Supplemental Figure 1. (A) The CASQ1 tail possesses only negative residues, mostly Asp and rarely Glu. Among mammalian species (shown in pink), the conservation is very high, only very rarely Glu is found and referred to as Dn-motif. The length of the Dn-motif decreased with evolution as fishes have the longest, mammals have the shortest and amphibians and reptiles have intermediate length. **(B)** The CASQ2 has longer tail that has non-negative residues like Asn, Gly, and Ser repeating after every few negatively-charged residues, Asp and Glu; therefore designated as DEXn-motif. Red indicates total conservation of the residue and cyan indicates conservative substitution of the residue. Unique residues that are not conserved are shown in bold font. The probability of disordered region dispersion in rat CASQ1 **(C)** and CASQ2 **(D)** sequences. All the prediction programs unanimously show that the C-terminus (Dn and DEXn motifs) of CASQ isoforms are intrinsically disordered regions, while the domain I, II and III regions of either isoform do not show high probability of intrinsically disorderedness. CASQ sequences from other organisms also show similar disordered pattern.
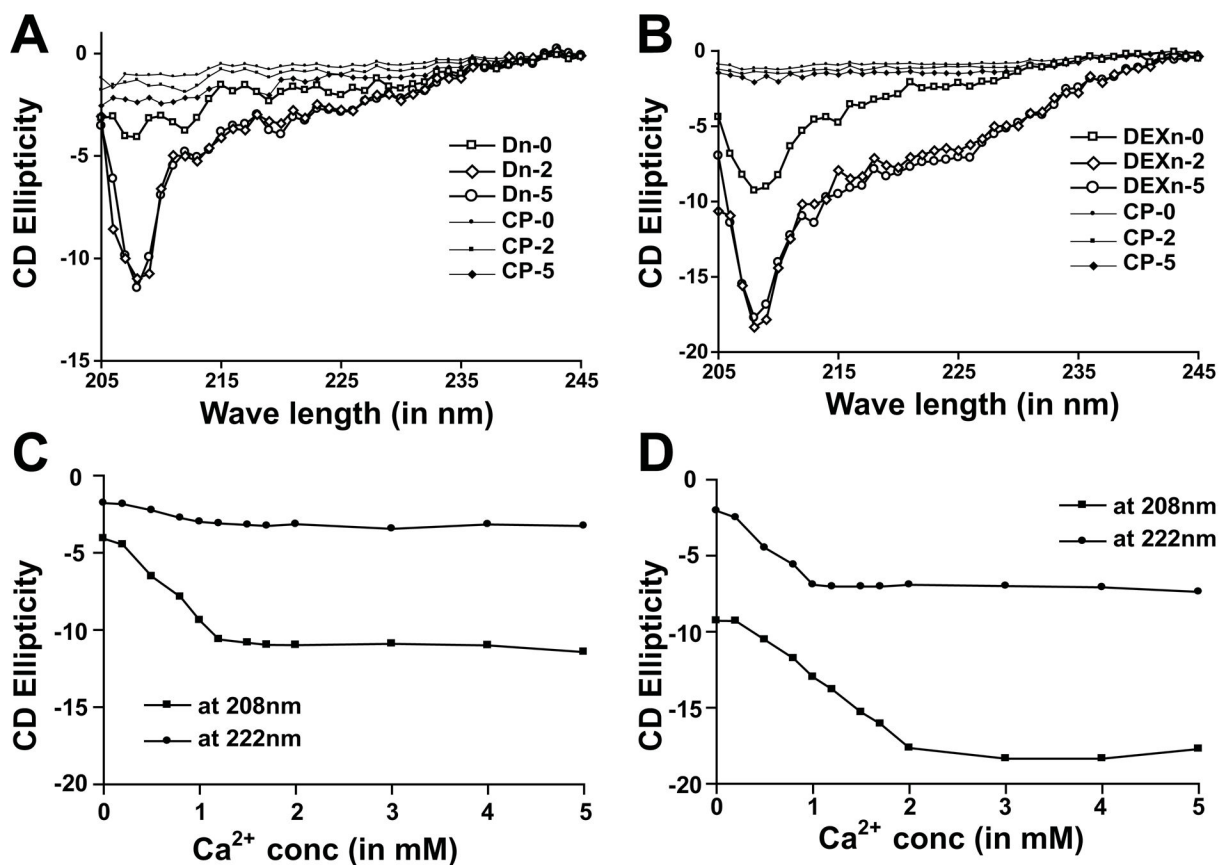
**Figure 2. Dn and DEXn motifs undergo distinct structural changes upon exposure to Ca$^{2+}$**
(**A**) Dn-motif peptide acquires coiling when Ca$^{2+}$-concentration is increased. At 0 mM Ca$^{2+}$ (Dn-0), the Dn-motif remains in almost linear conformation. In 2 mM and 5 mM Ca$^{2+}$ (Dn-2 and Dn-5 respectively) Dn-peptide shows marked increase in the negative ellepticity at 208 nm. (**B**) DEXn-motif peptide acquires helical content in addition to coiling upon Ca$^{2+}$-binding. At 0 mM Ca$^{2+}$ (DEXn-0), the DEXn-peptide remains in coiled conformation. In 2 mM and 5 mM Ca$^{2+}$ (DEXn-2 and DEXn-5 respectively) DEXn-peptide shows marked increase in the negative ellepticity both at 222 and 208nm. Plot of CD ellepticity at 208 and 222nm for Dn-peptide (**C**) and DEXn-peptide (**D**) with increasing Ca$^{2+}$-concentration. For the DEXn-peptide, the transition of helical content is achieved ~1 mM Ca$^{2+}$, while that of coiling is achieved ~2 mM Ca$^{2+}$. The Dn-peptide achieves the transition of coiling content ~1 mM Ca$^{2+}$. Control peptide is denoted as CP.
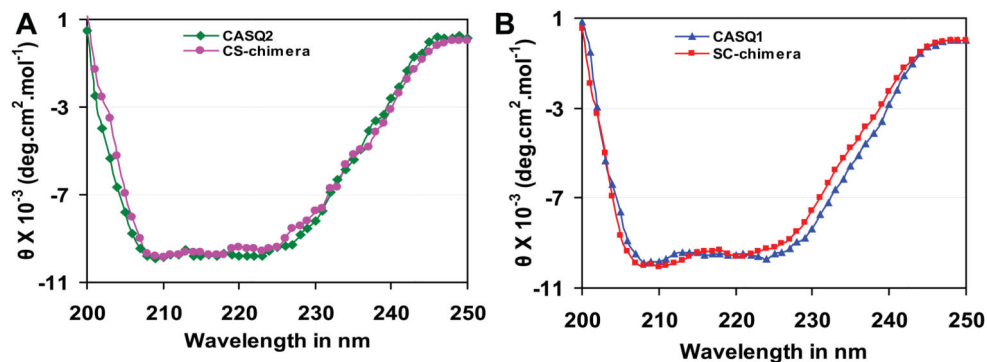
**Figure 3. Chimeric CASQ proteins can fold to similar conformation as the wildtype CASQ isoforms**

(**A**) Comparison of MRE between CASQ2 and CS-chimera calculated from the CD spectra. (**B**) Comparison of CD spectra of CASQ1 and SC-chimera. Both the chimeras have similar CD spectra indicating that the relative proportion of secondary structural content is unchanged.
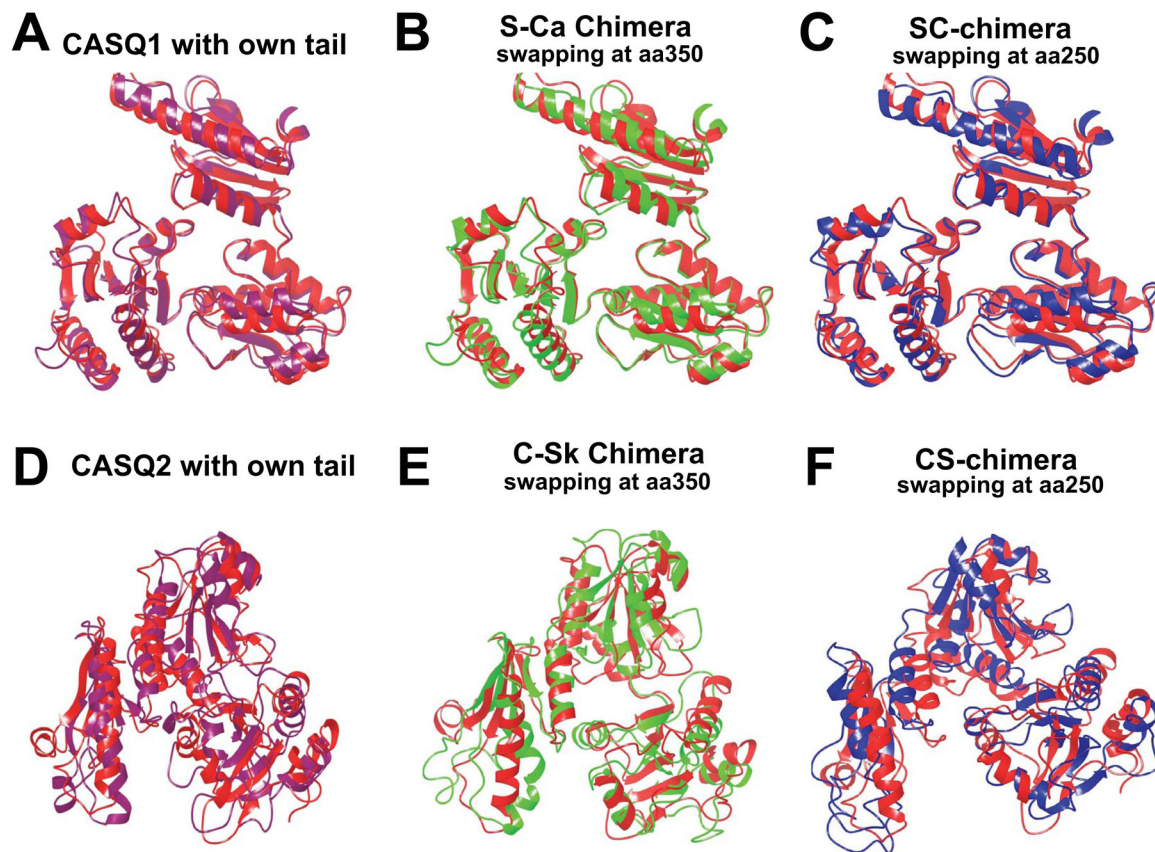
**Figure 4. Chimerization does not impair folding of either of the CASQ isoforms**
Superposition of the region (15–355 aa) of original structural file (PDB: 3TRQ) with that of
CASQ1 with its own C-terminal residues **(A)**, S-Ca chimera **(B)** and SC-chimera **(C)**.
Superposition image of the region (15–355 aa) of original structural file (PDB: 2VAF), with
that of CASQ2 with its own C-terminal residues **(D)**, S-Ca chimera **(E)** and SC-chimera **(F)**.
The original structural file in all the cases is shown in red. Both the chimeras are closely
superimposable on the respective WT structures. This computational data suggest that
swapping of residue from 250-to-350 has no drastic structural consequences.
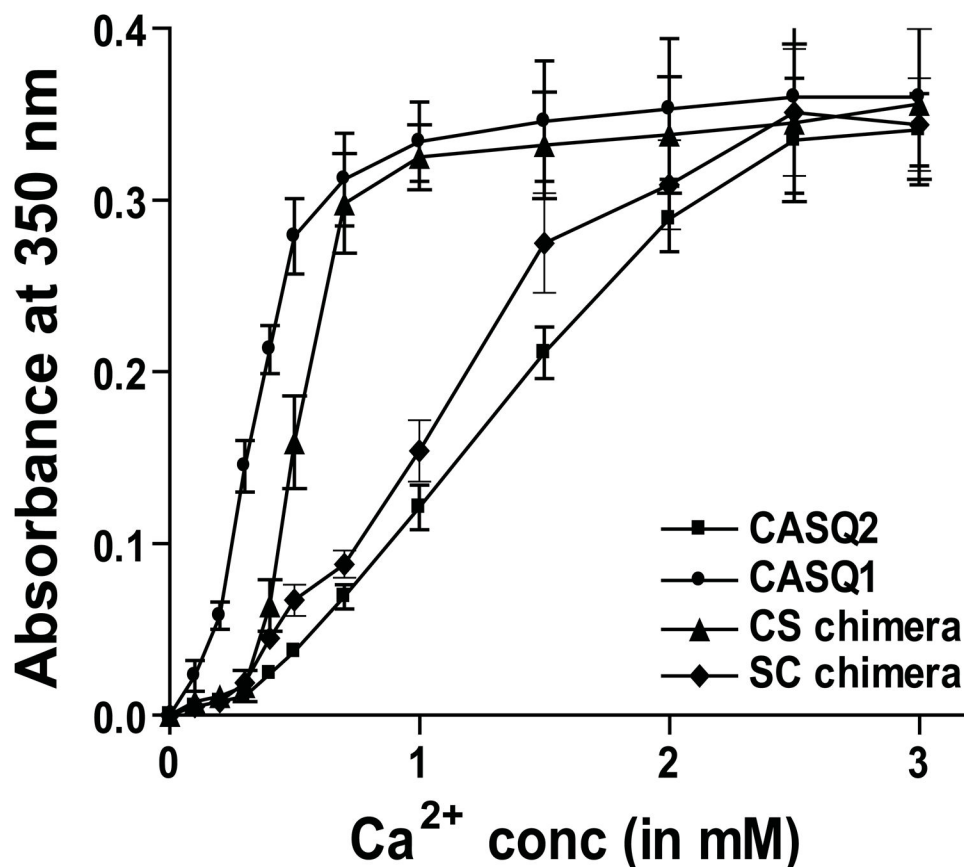
**Figure 5. Swapping of the C-termini reverses the polymerization properties of CASQ2 isoforms**
Addition of $Ca^{2+}$, to solution containing the CASQ1 shows increased turbidity even with 0.1 mM $Ca^{2+}$ and reaches saturation ~1 mM $Ca^{2+}$. Whereas, CASQ2 shows increased turbidity starting with ~0.3 mM reaching saturation ~2.25 mM $Ca^{2+}$. So, the CASQ1 polymerizes with less $Ca^{2+}$ than CASQ2. The CS-chimera follows the kinetics of CASQ1, while the SC-chimera follows that of the CASQ2. Therefore, the DEXn-motif being large causes structural hindrance to the formation of back-to-back tetramer (see Supplemental Figure 2) and can influence linear polymerization of CASQ2 as a rate-limiting step.